

The mass of the neutron star in the low-mass X-ray binary 2A 1822–371 *

P.G. Jonker^{1*}, M. van der Klis², P.J. Groot^{3,4}

¹*Institute of Astronomy, Madingley Road, CB3 0HA, Cambridge*

²*Astronomical Institute “Anton Pannekoek”, University of Amsterdam, Kruislaan 403, 1098 SJ Amsterdam*

³*Harvard-Smithsonian Center for Astrophysics, 60 Garden Street, Cambridge, MA 02138, USA*

⁴*Department of Astrophysics, University of Nijmegen, P.O.Box 9010, Nijmegen, The Netherlands*

2 July 2018

ABSTRACT

Using phase resolved spectroscopic observations obtained with the Ultraviolet and Visual Echelle Spectrograph on ESO’s Kueyen Very Large Telescope supplemented by spectroscopic observations obtained with the Boller and Chivens Spectrograph on the Walter Baade Magellan telescope, we found sinusoidal radial-velocity variations with a semi-amplitude 327 ± 17 km/s. From previous observations and from the fact that the epoch of minimum velocity arrived early with respect to the epoch calculated from pulse timing we know that the companion star is suffering from irradiation. Since we most likely observed primarily the side of the companion star facing the observer at phase ~ 0.75 the velocity quoted above is not the true radial velocity semi-amplitude of the companion star. Assuming a uniform contribution to the line profile from this hemisphere yields a radial velocity semi-amplitude of 280 ± 26 km s^{-1} for a systemic velocity of 54 ± 24 km s^{-1} ; if the contribution is instead weighted somewhat more towards the side of the companion facing the X-ray source then the true semi-amplitude is larger than this value. Together with the well constrained inclination ($81^\circ < i < 84^\circ$) and the mass-function determined from pulse-timing analysis ($2.03 \pm 0.03 \times 10^{-2} M_\odot$), we derive a lower limit to the mass of the neutron star and to that of the companion star of $0.97 \pm 0.24 M_\odot$ and $0.33 \pm 0.05 M_\odot$, respectively (1σ ; including uncertainties in the inclination). We briefly discuss other aspects of the spectrum and the implications of our findings.

Key words: stars: individual (2A 1822–371) — stars: neutron — X-rays: stars — techniques: radial velocities

1 INTRODUCTION

Low-mass X-ray binaries (LMXBs) are generally old ($> 10^8$ yr) binary systems in which a low-mass star ($\lesssim 1 M_\odot$) transfers matter to a neutron star or a black hole. The neutron star LMXBs are thought to be progenitors of millisecond radio pulsars. Due to accretion of matter and decay of the magnetic field during the LMXB-phase the neutron star spins-up to millisecond periods (Radhakrishnan & Srinivasan 1982; Alpar et al. 1982; see Bhattacharya 1995 for a review). To date, only eight out of several hundred LMXBs, among which three with millisecond periods, are known to show pulsations. Measuring Doppler delays of the pulse ar-

rival times allowed for an accurate measurement of both the orbital period and the size of the orbit of the neutron star in six cases (Her X-1, which is in fact an intermediate-mass X-ray binary, Tananbaum et al. 1972; GRO J1744–28, Finger et al. 1996; SAX J1808.4–3658, Chakrabarty & Morgan 1998; 2A 1822–371, Jonker & van der Klis 2001; XTE J1751–305, Markwardt & Swank 2002; XTE J0929–314, Galloway et al. 2002). The orbit of the companion star can be determined by observing periodic shifts in the central wavelengths of (absorption) lines in its stellar spectrum. If the orbital inclination is known, one can solve for the masses of the stellar components.

The initial mass of newly formed neutron stars is highly uncertain but theoretical calculations show that they most likely fall in a small range around $1.32 M_\odot$ (Timmes, Woosley & Weaver 1996; Fryer & Kalogera 2001 derived that 81–96 percent of the initial neutron star masses fall in

* email : peterj@ast.cam.ac.uk

*Based on observations made with ESO Telescopes at the Paranal Observatories under programme ID 267.D-5683

the range of 1.2–1.6 M_{\odot}). Theories on the equation of state (EoS) of neutron–star matter at supranuclear density provide a firm upper limit on the neutron star mass which is different for each EoS. Therefore, measuring a high mass for even one neutron star would imply the firm rejection of many proposed EoS (see discussion by van Paradijs & McClintock 1995). The measured masses of radio pulsars, including millisecond radio pulsars, are consistent with $1.4M_{\odot}$ (Thorsett & Chakrabarty 1999). Some theories explaining the presence of kHz quasi–periodic oscillations in accreting non–pulsating LMXBs (see van der Klis 2000 for a review) suggest a neutron star mass of $\sim 2M_{\odot}$.

The lightcurve of 2A 1822–371 shows clear signs of orbital modulation in both the X–ray and optical bands (e.g. partial eclipses and a sinusoidal modulation in optical and X–rays; White et al. 1981; Seitzer et al. 1979; Mason et al. 1980) with an orbital period of 5.57 hours. The implied inclination of 2A 1822–371 is $i = 82^{\circ} - 87^{\circ}$ (Hellier & Mason 1989). Heinz & Nowak (2001) used *ASCA* and *RXTE* data to model the lightcurve; they found $81^{\circ} < i < 84^{\circ}$. Recently, 0.59 s pulsations were discovered from this system and from pulse arrival time delay measurements it was found that the neutron star in 2A 1822–371 has an *asini* of 1.006 lightseconds (Jonker & van der Klis 2001). From eclipse and pulse timing an accurate ephemeris is known (Parmar et al. 2001; Jonker & van der Klis 2001). Clearly, spectroscopic measurements of the radial velocity curve of the companion are indicated at this stage in order to check on the mass of the neutron star.

Cowley, Crampton, & Hutchings (1982) detected weak absorption lines in the spectrum of 2A 1822–371 ($H\delta$, $H\gamma$, and some HeI absorption lines) but due to the lack of signal–to–noise a radial velocity could not be measured. Later, Harlaftis, Charles, & Horne (1997) measured the radial velocity of the companion in 4U 1822–37 using the He I absorption line at 5875.966Å. The presence of an extra absorption component in the same part of the spectrum and the relatively low resolution ($\sim 75 \text{ km s}^{-1}$ for $H\alpha$) which kept them from resolving the two components, yielded a lower limit on the radial velocity of the companion star and mass of the neutron star of 225 km s^{-1} and $0.6_{-0.3}^{+1.0}M_{\odot}$, respectively.

In this Letter we report on the spectroscopic observations of 2A 1822–371 obtained with the Ultraviolet and Visible Echelle Spectrograph on ESO’s 8.2-m Kueyen Very Large Telescope and on spectroscopic observations obtained with the Boller and Chivens Spectrograph on the 6.5-m Walter Baade Magellan Telescope.

2 OBSERVATIONS AND ANALYSIS

2A 1822–371 was observed with the Ultraviolet and Visible Echelle Spectrograph (UVES) mounted on the Kueyen Very Large Telescope (VLT) from UT 00:51–07:10 July 20, 2001 (HJD 2452110.546–2452110.808). Due to a technical problem with the telescope no observations were obtained from UT 05:27–06:20; this led to a gap in the coverage of the binary orbit from phase 0.38 to 0.50. The integration time was 900 s. UVES was operated in its 390+564 standard mode with a slit width of 1 arcsecond. This yielded spectra with a resolution of $\sim 0.1\text{Å}$ per pixel. The night was photometric

with a seeing less than 1 arcsecond. Thorium–Argon lamp spectra were obtained after each observing block of one hour.

Spectroscopic observations with the Walter Baade Magellan Telescope were obtained on June 30 (UT 01:48–09:28; HJD 2452090.584–2452090.896), July 1 (UT 03:17–09:39; HJD 2452091.646–2452091.904), and July 2 (UT 03:22–09:25; HJD 2452092.649–2452092.894) 2001 using the Boller and Chivens Spectrograph. The slit–length and width were 72 and 0.75 arcseconds, respectively, providing a resolution of 0.9Å per pixel. The integration time was 600 s. Helium–Argon lamp spectra were obtained approximately every hour. The spectra were bias–subtracted, flatfielded, extracted using the ECHELLE (VLT) and SPECRED (Magellan) reduction packages and fitted with routines in the STSDAS package in IRAF[†].

UVES spectra were extracted from 3700–4500Å, 4640–5580Å, and 5670–6660Å. The rms scatter of the wavelength calibration obtained by applying a fourth order polynomial fit to the wavelengths of more than 50 lamp lines was $\sim 0.003\text{Å}$. The source spectra were rebinned to a resolution of $\sim 0.3\text{Å}$. The normalisation of the spectra occurred in three stages. First, for each order, the average blaze profile was determined by fitting a cubic spline to the average spectrum of all observations combined. The regions where lines were known to be present from previous spectroscopic observations of the source (see Section 1) were masked during the fit. Second, each order, for each spectrum, was divided by this fit. Finally, all orders were combined and scaled to a mean level of 1.

The Magellan spectra cover 5310Å–6300Å. The wavelength calibration was obtained from a second order polynomial fit to 12 lamp lines (rms of $\sim 0.05\text{Å}$). A second order cubic spline fit to the continuum was used to take out the instrumental profile and normalise the spectrum.

Using the ephemeris provided by the pulse timing (Jonker & van der Klis 2001) we determined the phase at the centre of each spectrum. The Magellan observations falling in the same phase bin (bin–width 0.03) were averaged to increase the signal–to–noise. The error in the phase is dominated by the integration time used to obtain the spectrum and/or the spread in phase when averaging the Magellan data, and not by the propagation of the ephemeris to the date of the observation. Phase zero is defined as superior conjunction of the neutron star (X–ray eclipse).

3 RESULTS

In Figure 1 we show as an example the full UVES spectrum at orbital phase 0.67 ± 0.02 rebinned to a wavelength resolution of 0.6Å . Since the spectra are varying strongly as a function of orbital phase, we were not able to cross–correlate the spectra in order to determine the radial velocity. Instead, we fitted Gaussians to the line profiles and compared the central wavelength with the rest wavelength of the line. Fitting was done using a downhill simplex method (AMOEBA; Press et al. 1992) and errors on the parameters were determined using an independent Monte Carlo resampling technique.

[†] IRAF is distributed by the National Optical Astronomy Observatories

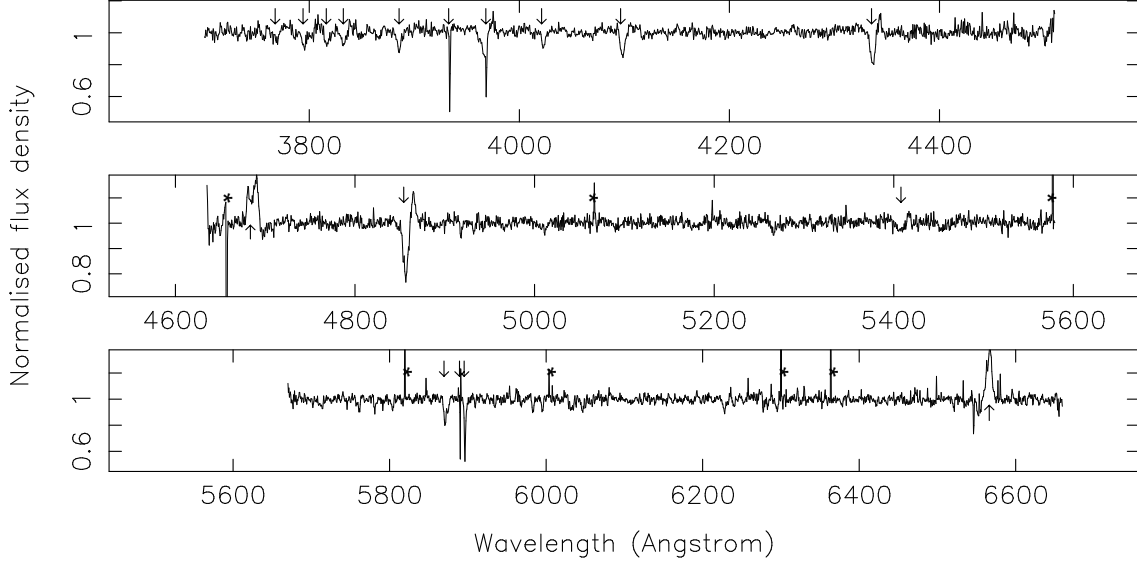


Figure 1. Total spectrum at phase 0.67 ± 0.02 rebinned to a wavelength resolution of 0.6 \AA . The $H\epsilon$, $H\theta$, $H\eta$, $H\zeta$, $H\epsilon$, $H\delta$, $H\gamma$, $H\beta$ hydrogen Balmer lines, the double-peaked He II and $H\alpha$ emission lines, and the He I absorption lines at 4026.357 \AA and 5875.966 \AA are clearly visible. The most prominent lines have been indicated with an arrow, whereas noise spikes due to residual cosmics or CCD imperfections have been indicated with a star.

Table 1. Overview of the detected lines. In the last column the range in phase over which the line was predominantly detected is given.

Element	Rest wavelength (\AA)	Absorption (A)/emission (E)	Present at phases
$H\epsilon$	3770.630	A	0.55-1
$H\theta$	3797.898	A	0.55-1
He I	3809.10	E	0.2-0.35, 0.65-1
$H\eta$	3835.384	A	0.55-1
He I	3888.60	E	0.9-1, 0-0.1
$H\zeta$	3889.049	A + E (sometimes double)	0.55-1
Ca II	3933.663	A interstellar	0-1
Ca II	3968.468	A interstellar	0-1
$H\epsilon$	3970.072	A + E (sometimes double)	0.5-1
He I	4026.357	A	0.3-1
$H\delta$	4101.734	A + E (sometimes double)	0.55-1
$H\gamma$	4340.464	A + E (sometimes double)	0.55-1
He II	4685.71	E double	0-1
$H\beta$	4861.325	A + E (sometimes double)	0.5-1
He II	5411.53	E	0.95-1, 0-0.1
He I	5875.966	A	0.5-1
Na D	5889.951	A interstellar	0-1
Na D	5895.924	A interstellar	0-1
$H\alpha$	6562.80	E double	0-1

We detected several lines of the hydrogen Balmer series (among which the double-peaked $H\alpha$ emission line). Their profiles varied as a function of orbital phase. To show the variability of the hydrogen absorption lines in more detail we plotted a blow-up of the region of $H\beta$ as a function of phase in Figure 2 (*left panel*). $H\beta$ changed from a double-peaked emission line into a strong absorption line with a single emission line on the red side, and back into a strong double-peaked emission line with a weak absorption to the blue side. This pattern is detected in the two strongest hydrogen Balmer absorption lines ($H\beta$ and $H\gamma$). Hints of the

presence of the same pattern were found for the weaker hydrogen Balmer lines below 4000 \AA as well, but due to the limited signal-to-noise the presence or absence of such components could not always be determined. These double-peaked lines are most likely formed in the optically thin outer parts of the accretion disk.

Several He I lines were detected (e.g. the He I 5875.966 \AA absorption line also reported by Harlaftis, Charles & Horne 1997, the He I 4026.357 \AA absorption line and the He I 3809.10 \AA and 3888.60 \AA emission lines). The He I lines did not show evidence for changes in line-profile such as

those found for the hydrogen Balmer lines, although since the lines are often weak we cannot always exclude that the lines are composites of lines originating both in the accretion disk and in the secondary star. The Bowen blend, detected in 2A 1822–371 by Mason & Cordova (1982) was not clearly detected because it fell close to the edge of the CCD. Double-peaked He II emission lines with rest wavelength of 4685.71Å and 5411.53Å were also detected. Their strength and profile changed strongly as a function of orbital phase, similar to the double-peaked H β and H γ lines. A list of lines which were clearly detected is given in Table 1.

For our radial velocity study we only used the He I absorption lines at 4026.357Å and 5875.966Å (see Figure 2; *right panel*; dots are measurements using VLT data and crosses are measurements using Magellan data. Note that the two sets of measurements are completely consistent without any evidence for a systematic offset.) We excluded the hydrogen Balmer lines since we could not always unambiguously separate the emission component(s) from the absorption component. When the hydrogen absorption and emission components could unambiguously be separated the velocities determined from the hydrogen absorption lines were consistent with those of the He I absorption lines. The He I lines were always detected at phases 0.3 to 0.95. We fitted a sinusoid to the measured radial-velocity curve using the orthogonal distance regression (ODR) technique to minimize the χ^2 (the reported errors indicate the 1σ uncertainties throughout this paper).

Fixing the orbital period and phase to the values predicted from pulse timing did not result in a good fit ($\chi^2 = 436$ for 45 degrees of freedom). Inspection of the fit reveals that the phase of minimal velocity occurs earlier than expected on the basis of the orbital ephemeris (see Figure 2; *right panel* dotted line). Such effects have been noticed before in radial velocity curves of several Cataclysmic Variables (CVs; e.g. Davey & Smith 1992) and are thought to be caused by asymmetric heating of the companion star; i.e. the centre of light is offset from the centre of mass of the secondary, and not on the binary axis. Since one side of the companion star contributes disproportionately, the rotational broadening of the absorption profile is not uniform; this leads to a systematic velocity shift (Wade & Horne 1988). We will come back to this in the Discussion. This heating effect can be accommodated by allowing for a phase shift in the sinusoid or by introducing a small apparent eccentricity (Davey & Smith 1992).

Leaving the phase of the sinusoid as a free parameter improved the fit dramatically ($\chi^2 = 90$ for 44 degrees of freedom; see Figure 2, *right panel*, solid line; the phase shifts from 0.0 to -0.08 ± 0.01). This yields a systemic velocity, v_{sys} , of 67 ± 15 km s $^{-1}$ and a radial velocity semi-amplitude, K , of 327 ± 17 km s $^{-1}$. We note that the v_{sys} and K are correlated in the fit since the absorption line measurements are predominantly located at phases 0.5 to 1. After Davey & Smith (1992) we tried to improve the fit by including the second harmonic of the sinusoid to accommodate a small, apparent, eccentricity. The fit with two sinusoids was not significantly better (cf. $\chi^2 = 82$ for 42 degrees of freedom for a two-sinusoids fit vs. $\chi^2 = 90$ for 44 degrees of freedom for a single sinusoid fit).

4 DISCUSSION

We determined the radial velocity of the companion star of 2A 1822–371 using VLT and Magellan spectroscopic observations. Fitting a sinusoid to radial velocity measurements using two He I stellar absorption lines a semi-amplitude of 327 ± 17 km s $^{-1}$ was found, with a best fit systemic velocity of 67 ± 15 km s $^{-1}$. We could combine this with the velocity amplitude of the neutron star (derived from pulse-timing analysis; Jonker & van der Klis 2001) to derive a neutron and companion star mass. However, we found that the epoch of minimum velocity occurs early with respect to the epoch calculated from the ephemeris derived from pulse timing. Together with the fact that the absorption lines were predominantly detected around phase 0.75 this is strong evidence that the companion star suffers from asymmetric heating (see also Davey & Smith 1992; that 2A 1822–371 suffers from X-ray heating was also shown by Cowley, Crampton & Hutchings 1982 and Harlaftis, Charles & Horne 1997). Therefore, it is likely that the centre-of-light of the companion star does not coincide with its centre of mass, nor with the binary axis.

The effect this has on the determined radial velocity amplitude depends on what part of the companion star is observed and whether as assumed here and below the companion star is in co-rotation. In several CVs absorption lines from the non-irradiated side of the companion star, the side pointing towards the observer at phase 0 (for an inclination, i , of 90°) are observed (Wade & Horne 1988). In that case the measured radial velocity amplitude is an upper limit to the true amplitude. If we were to observe the irradiated side in such a case the determined radial velocity amplitude would be a lower limit. Furthermore, the minimum and maximum of the radial velocity curve would both move closer to phase 0.5 whereas the velocities at phase 0 and 0.5 should be the same (and they should be zero). However, from Figure 2 (*right panel*) it is clear that in case of 2A 1822–371 these velocities are unequal and thus this model is not applicable here.

The distribution of points in Figure 2 (*right panel*) indicates that the leading side of the companion star was observed predominantly, i.e., the side pointing towards the observer at phase 0.75 ($i = 90^\circ$). If we assume a uniform contribution from this leading hemisphere to the line profiles, then, due to the rotation of the companion star, the velocities at phase 0 and 0.5 will be red and blue shifted, respectively, but the magnitude of the shift will be the same. The velocity measured at phase 0.25 and 0.75 with respect to the average of the velocities at phase 0 and 0.5 (which is the systemic velocity) represents the true radial velocity amplitude in such a model. Since only part of the sinusoid is observed in case of 2A 1822–371 the radial velocity semi-amplitude is calculated from the difference between the average of the velocities at phases 0 and 0.5, and the velocity at 0.75 only. Using this model we derive a systemic velocity of 54 ± 24 km s $^{-1}$ and a radial velocity semi-amplitude of 280 ± 26 km s $^{-1}$. Combining this with the velocity amplitude of the neutron star a neutron star mass of $0.97 \pm 0.24 M_\odot$ is found (1σ ; the uncertainty in the system inclination, $i = 82.5^\circ \pm 1.5^\circ$, was included; for the determination of the inclination see references given in the Introduction). The companion star mass is $0.33 \pm 0.05 M_\odot$ for $i = 82.5^\circ \pm 1.5^\circ$.

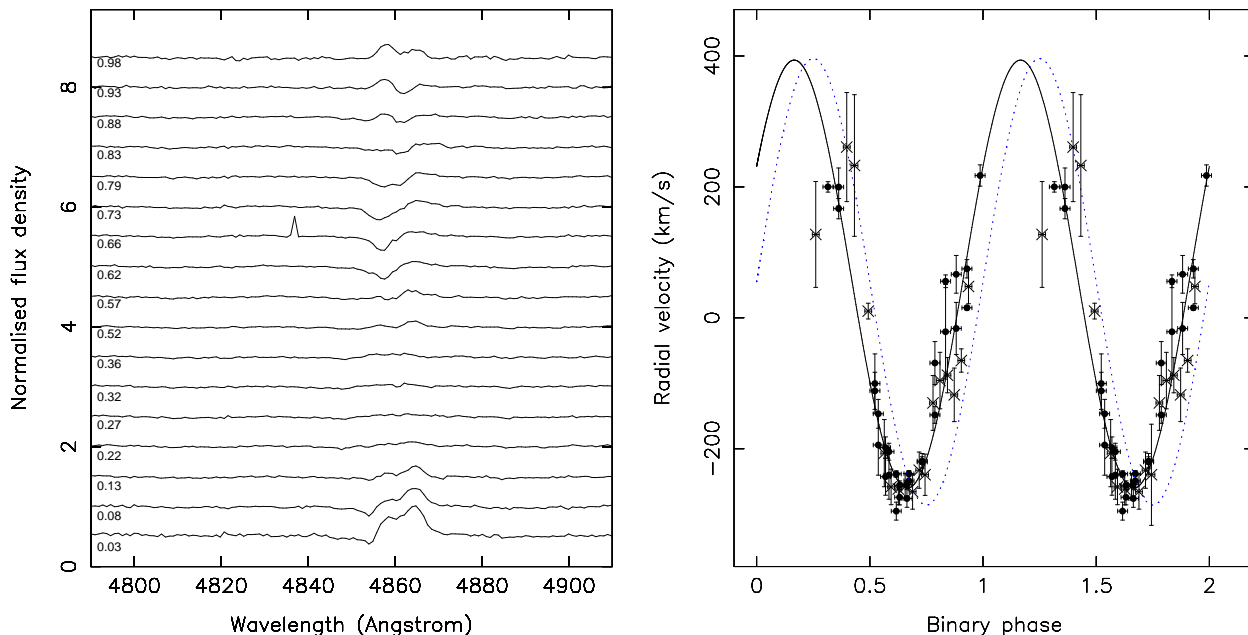


Figure 2. *Left:* The changing profile of H β as a function of binary orbital phase. The phase is given by the number on the left in the plot. The spectra have been shifted by 0.5 units in flux for clarity. *Right:* The radial velocity as a function of binary orbital phase determined from the He I 4026.357 Å and 5875.966 Å absorption lines. The dots are the measurements using the VLT data and the crosses those of the Magellan data. For clarity two cycles have been plotted. The best-fit sinusoid as well as the fit with the phase of the sinusoid fixed to the value expected from the pulse-timing ephemeris are overplotted (solid line and the dotted line, respectively).

If instead the orientation of the hemisphere we observe is, as the data suggest, somewhat more towards the side facing the X-ray source, then these quoted values of K and the masses are likely to be underestimates. Clearly, phase-resolved observations detecting lines from the cold hemisphere of the companion star are needed in order to investigate the systematic effects further. We note however that radial velocity measurements using lines from the non-irradiated side only would lead to an upper limit on the mass of the neutron star. Thorsett & Chakrabarty (1999) determined that the masses of neutron stars in radio pulsar binaries are consistent with a Gaussian distribution around $M = 1.35 \pm 0.04 M_{\odot}$. The lower limit to the mass of the neutron star in 2A 1822–371 is consistent with this within 2σ .

Naylor et al. (1988) observed several He I absorption lines among which the two we observed in 2A 1822–371 in the spectrum of the source AC 211 in M 15 (the source is thought to be in the class of Accretion Disk Corona, ADC, sources of which 2A 1822–371 is the prototype; White et al. 1981). They argue that the He I absorption in AC 211 is due to disk edge material, which when illuminated by the hot inner part of the accretion disk gives rise to the He I absorption lines. Unexplained in such a scenario is the fact that even at orbital phases where the inner part of the accretion disk is not observed through localized disk edge material (e.g. at phases 0.2–0.7) still absorption lines are observed. Furthermore, they argue that the radial velocity measurements using these lines in AC 211 reflect the orbital motion of the compact object. In case of 2A 1822–371 we know from the pulse timing measurements of the orbit of the neutron star that this is not the case.

As for several CVs (most notably U Gem; Davey &

Smith 1992), the observed, irradiated, side of the companion star seems not centred towards the neutron star or white dwarf in the case of CVs. The reason for this is unclear. It has been speculated that the hot spot plays an important role in heating the companion star in CVs (Davey & Smith 1992). However, as for CVs (Smith 1995) this seems unlikely in case of 2A 1822–371 since the centre of the accretion disk and the neutron star in LMXBs such as 2A 1822–371 should be much brighter than the hot spot. Even though shielding of the companion star by the accretion disk could be important the large ADC should circumvent shielding at least partially. Modelling irradiation-induced motions in the secondary stars in CVs Martin & Davey (1995) showed that the heated material is deflected towards the leading hemisphere as a result of the Coriolis force; this is in accordance with our findings (see Smith 1995 for a review).

Comparing our data with previous spectroscopic observations (Charles, Barr & Thorstensen 1980; Cowley, Cramp-ton & Hutchings 1982; Mason et al. 1982; Harlaftis, Charles & Horne 1997) we note that Harlaftis, Charles & Horne (1997) measured the He I 5875.966 Å line to be present over the whole orbit. Furthermore, a separate absorption component arose near phase 0.0–0.2. In our higher resolution UVES data we did not find evidence for this extra component, nor were we able to measure the He I line at all phases. Mason et al. (1982) already pointed out that the spectra showed evidence for long term variability. With our new high-resolution UVES spectra we can settle the issue of the presence of emission or absorption lines in the blue part of the spectrum (see Discussion in Mason et al. 1982); we now know that at certain phases both (He I) emission and hydrogen Balmer absorption lines are present.

As was noted before, for a neutron star mass of $\sim 1.4 M_{\odot}$

the companion star is undermassive, i.e. less massive than a main-sequence companion star filling its Roche-lobe in a 5.57 hour orbit (main-sequence mass $\sim 0.62 M_{\odot}$; e.g. Mason et al. 1982; Cowley, Crampton & Hutchings 1982; Jonker & van der Klis 2001). Thus the density of the star, like that of evolved stars, is lower than the density of a main-sequence star. The companion stars in some CVs were also shown to be undermassive. It is believed that the companion star in those CVs is out of thermal equilibrium (see Beuermann et al. 1998). However, if the companion star in 2A 1822–371 is evolved this would mean that it was considerably more massive than $0.4 M_{\odot}$ at the onset of mass transfer since such a star would not have evolved in a Hubble time. Alternatively, a scenario in which the companion star was brought into contact with its Roche lobe by transfer of angular momentum due to gravitational radiation can be envisaged. However, such losses are not sufficient to sustain the mass transfer rate of $\sim 2 \times 10^{-9} M_{\odot} \text{yr}^{-1}$ which is needed to explain the intrinsic X-ray luminosity ($L_X \sim 2 - 4 \times 10^{37} \text{ergs}^{-1}$; Jonker & van der Klis 2001). Since X-ray irradiation of the companion star was shown to heat the star, irradiation induced mass-transfer (Ruderman et al. 1989) could in principle also help to keep mass-transfer going. However, due to the presence and size of a bulge on the accretion disk edge a large fraction of the companion star will be shielded and the irradiating flux will be reduced, making it unlikely that a mass transfer rate of $\sim 2 \times 10^{-9} M_{\odot} \text{yr}^{-1}$ is induced by X-ray irradiation. In addition to gravitational radiation and X-ray irradiation angular momentum transferred by magnetic braking (Verbunt & Zwaan 1981) could explain the mass-loss rate (although it was found that at present the orbit is expanding; Parmar et al. 1986). We conclude therefore that the companion star in 2A 1822–371 is either out of thermal equilibrium (possibly due to the high mass loss rate and effects of X-ray heating), or evolved and has lost more than $\sim 0.4 M_{\odot}$ (this would make the companion star $\sim 0.8 M_{\odot}$ at the start of mass transfer; such a star could just have evolved in a Hubble time), or an interplay between angular momentum losses caused by magnetic braking and gravitational radiation supplemented by mass-loss driven by X-ray irradiation is driving the evolution of this LMXB.

ACKNOWLEDGMENTS

PGJ is supported by EC Marie Curie Fellowship HPMF-CT-2001-01308. MK is supported in part by a Netherlands Organization for Scientific Research (NWO) grant. PGJ would like to thank Gijs Nelemans for numerous useful discussions. The authors would like to thank the referee for his/her comments and suggestions which helped improve the paper.

REFERENCES

- Alpar M. A., Cheng A. F., Ruderman M. A., Shaham J., 1982, *Nat*, 300, 728
- Beuermann K., Baraffe I., Kolb U., Weichhold M., 1998, *A&A*, 339, 518
- Bhattacharya D., 1995, *Millisecond pulsars*, eds Lewin, van Paradijs, van den Heuvel. ISBN 052141684, Cambridge University Press, 1995.
- Chakrabarty D., Morgan E. H., 1998, *Nat*, 394, 346
- Charles P., Barr P., Thorstensen J. R., 1980, *ApJ*, 241, 1148
- Cowley A. P., Crampton D., Hutchings J. B., 1982, *ApJ*, 255, 596
- Davey S., Smith R. C., 1992, *MNRAS*, 257, 476
- Finger M. H., Koh D. T., Nelson R. W., Prince T. A., Vaughan B. A., Wilson R. B., 1996, *Nat*, 381, 291
- Fryer C. L., Kalogera V., 2001, *ApJ*, 554, 548
- Galloway D. K., Morgan E. H., Remillard R. A. g., Chakrabarty D., 2002, *IAU Circ*, 7900, 2+
- Harlaftis E. T., Charles P. A., Horne K., 1997, *MNRAS*, 285, 673
- Heinz S., Nowak M. A., 2001, *MNRAS*, 320, 249
- Hellier C., Mason K. O., 1989, *MNRAS*, 239, 715
- Jonker P. G., van der Klis M., 2001, *ApJ*, 553, L43
- Markwardt C. B., Swank J. H., 2002, *IAU Circ*, 7867, 1+
- Martin T. J., Davey S. C., 1995, *MNRAS*, 275, 31
- Mason K. O., Cordova F. A., 1982, *ApJ*, 262, 253
- Mason K. O., Seitzer P., Tuohy I. R., Hunt L. K., Middleditch J., Nelson J. E., White N. E., 1980, *ApJ*, 242, L109
- Mason K. O., Murdin P. G., Tuohy I. R., Seitzer P., Branduardi-Raymont G., 1982, *MNRAS*, 200, 793
- Naylor T., Charles P. A., Drew J. E., Hassall B. J. M., 1988, *MNRAS*, 233, 285
- Parmar A. N., White N. E., Giommi P., Gottwald M., 1986, *ApJ*, 308, 199
- Parmar A. N., Oosterbroek T., Del Sordo S., Segreto A., Santangelo A., Dal Fiume D., Orlandini M., 2001, *A&A*
- Press W. H., Teukolsky S. A., Vetterling W. T., Flannery B. P., 1992, *Numerical recipes in FORTRAN. The art of scientific computing*. Cambridge: University Press, —c1992, 2nd ed.
- Radhakrishnan V., Srinivasan G., 1982, *Curr. Sci*, 51, 1096
- Ruderman M., Shaham J., Tavani M., Eichler D., 1989, *ApJ*, 343, 292
- Seitzer P., Tuohy I. R., Mason K. O., Middleditch J., Nelson J., White N. E., 1979, *IAU Circ*, 3406, 1+
- Smith R. C., 1995, *Secondary stars and irradiation*. ASP Conference Series, —Vol 85, 1995, D.A.H. Buckley and B. Warner, eds.
- Tananbaum H., Gursky H., Kellogg E. M., Levinson R., Schreier E., Giacconi R., 1972, *ApJ*, 174, L143
- Thorsett S. E., Chakrabarty D., 1999, *ApJ*, 512, 288
- Timmes F. X., Woosley S. E., Weaver T. A., 1996, *ApJ*, 457, 834+
- Verbunt F., Zwaan C., 1981, *A&A*, 100, L7
- Wade R. A., Horne K., 1988, *ApJ*, 324, 411
- White N. E., Becker R. H., Boldt E. A., Holt S. S., Serlemitsos P. J., Swank J. H., 1981, *ApJ*, 247, 994